# Comparison Between Mono- And Bi-Cortical Pins Of Unilateral-Uniplanar External Fixator In Tibial Diaphyseal Fracture Healing: Numerical Investigations

**Targol Bayat**
Ferdowsi University of Mashhad
**Yousof Mohandes** ( yousofmohandes@gmail.com )
Shiraz University of Medical Sciences
**Masoud Tahani**
Ferdowsi University of Mashhad
**Mohammad Tahami**
Shiraz University of Medical Sciences

**Research Article**

**Keywords:** Tibial diaphyseal fracture, Unilateral-uniplanar external fixator, Mechano-biology of bone healing, Mono-cortical pins, Bi-cortical pins

**Posted Date:** March 10th, 2022

**DOI:** https://doi.org/10.21203/rs.3.rs-1428537/v1

# Abstract

**Background:** This comparative study simulates bone healing outcomes around tibial diaphyseal fractures under unilateral uniplanar external fixators and compares mono-cortical pins and bi-cortical ones for fixation.

**Methods:** Eight finite element models of the fractured tibia-fixator constructs with 1 to 4 mono- or bi-cortical pins per bone segment were designed. A proven mechano-regulation algorithm was applied to the callus at the early stages of healing. Tissue differentiation was predicted, and axial stiffness was obtained to evaluate the healing process. To validate the simulation, finite element analysis of the models was compared with in-vitro biomechanical study results, and the error was less than 5%.

**Results:** The overall axial stiffness of the bone-fixator structure reached 885, 913, and 925 N/mm for the 4, 6, and 8 bi-cortical pins, respectively, which was very close to the results of mono-cortical pins (882, 893, and 916 N/mm). The average Young's modulus of callus elements for structures with both types of pins was about 4.4 MPa, which at the initial stage of healing resulted in all structures of fibrous callus. This result was consistent with all previous studies.

**Conclusions:** The healing simulation outcome in this study suggested that fixtures with mono-cortical pins resulted in fewer devastating complications and can be used as an alternative to the ones with bi-cortical pins.


# 1. Background

Tibial fracture accounts for a significant proportion of the long bone fractures, a high percentage of which occurs as open fractures (1, 2). Surgical interventions for fixating these fractures should overcome many challenges raised due to the risk of implant failure, infection, instability, bone malalignment, impaired healing, and refracture after implant removal (3). External fixation is among the common osteosynthesis modalities employed to anatomically align and stabilize open and severe closed fractures (4–6). This is suitable for people with unstable fractures and patients who cannot endure an open procedure or suffer from hemodynamically unstable conditions (2). Since the external fixators are placed outside the extremity, their geometry can be simple and resolve the need for perfect anatomic contouring (7). Furthermore, the fracture could be immobilized without the need for open reduction (8). Thus, the incision made during the surgery is limited, and the blood supply to the fracture site is less disturbed than the time an internal fixator is used (9). Moreover, surgeons can control the fixator stiffness by adding, removing, or loosening clamps to acquire desirable structural properties and subsequent favorable healing throughout the post-operative period (10, 11).

The most common type of external fixator for treating long bone fractures is the unilateral-uniplanar frame, which includes a side connecting rod with bi-cortical Schanz pins and clamps (8, 12). Bi-cortical Schanz pins penetrate both the near and far bone cortices, which, passing through the medullary canal, cause damage to its vascular net (4). In bicortical fixation, while drilling the far cortex, the threads of the

self-drilling pins may destroy the bone thread that has already been prepared in the near cortex (13). Besides, bi-cortical pins make secondary surgeries problematic for cases with a two-step surgery scenario. The primary external fixation is followed by internal fixation via plating or intramedullary nailing as the definitive treatment in these emergency cases. For the second surgery, bi-cortical pins must be backed out to let intramedullary nail pass through the medullary canal; thus, the risks of pin loosening and infection are increased (8).

The differentiation of connective tissues formed during the secondary healing process was predicted by several theories, in which two stimuli have been used to study the distribution of callus tissue. One is related to volumetric change and the other is related to change in shape. By comparing these theories, Isaksson et al. (14) proved that the mechano-regulation algorithm using deviatoric strain alone is effective for this prediction under axial loading. Therefore, the same method has been used in this research.

Previous studies have compared near- and far-cortex pin engagement effects in the structural strength, static and dynamic stability of the bone-external fixator construct (4, 8, 15, 16). Varady et al. (8) used porcine tibiae and showed that the mono-cortical fixation system performed comparably to the bi-cortical systems in terms of stiffness. Park et al. (16) employed synthetic bone and concluded that the mono-cortical pin system considerably increased fracture stability under axial compressive and torsional loads, compared to the bi-cortical pin one. Also, Greinwald et al. (17) used porcine bone specimens to determine bone temperature during pin penetration, which resulted in mono-cortical pins reducing the risk of thermal damage to both the surrounding tissue and the bone itself.

Despite many efforts, quantitative mechano-biological studies of the external fixation under different pin-bone anchorage have not been investigated. Therefore, the objective of the present study was to evaluate the healing outcome of unilateral-uniplanar external fixator of various pin arrangements fixed by mono-cortical or bi-cortical pins in the treatment of the tibial diaphyseal fracture. Considering the unique results of this article, the side effects of using bi-cortical pins can be avoided. To this end, by employing finite element-based computational modeling, a mechano-regulatory algorithm of bone healing was adopted to predict tissue differentiation within the fracture gap at the early phase of the repairing process.

# 2. Results

## 2.1. Model validation

The mean axial stiffness in the practical work of Ang et al. (9) was 528 N/mm and in the finite element (FE) model of this study was 554,407 N/mm. Considering a negligible difference between the experimental setup and the present FE model, the global stiffness in our computational analysis corresponded well to the empirical finding (9) with a deviation below 5%.

## 2.2. Axial stiffness

The axial stiffness of the bone-external fixator construct for BiC and MoC fixation groups is demonstrated in Fig. 1 for a similar number of pins ($X = constant$). The axial stiffness in the BiC group is slightly higher than that attained with the equivalent model in the MoC fixation. The mono-cortical external fixator reached the lowest axial rigidity using two pins ($X = 2$). Furthermore, it was found that the axial stiffness increased with the number of pins considerably when moving from $X = 2$ to $X = 4$ pins.

## 2.3. The average Young's modulus

The element-wise Young's moduli resulted at the initial stage of healing averaged over the callus domain in different FE models are shown in Fig. 2. Eavg in the BiC group is higher than the MoC group for each $X$. For both BiC and MoC groups investigated, increasing the number of pins caused $E_{avg}$ to rise in the callus. The highest $E_{avg}$ was found in the 8BiC configuration, while the lowest $E_{avg}$ was attributed to the 2MoC configuration.

## 2.4. The pattern of tissue differentiation

During the early stages of bone repair, healing domains in all numerical model variations were turned into tissue with Young's moduli between 1 and 5 MPa, corresponding to the range of fibrous tissue phenotype (Fig. 3). For all the configurations investigated, Fig. 3 discloses that highest and lowest Young's modulus regions were produced at the near and far cortex, respectively.

The deformed shape of the bone-fixator structure due to axial force with a scaling factor of 11 is shown in Fig. 4. For all specimens, the displacement of the fracture site toward the far cortex is greater than that of the near cortex, which affects the callus tissue differentiation.

## 2.5. The uniformity of tissue differentiation

The uniformity in tissue differentiation was evaluated by calculating the difference between the maximum ($E_{max}$) and minimum ($E_{min}$) Young's moduli at the repair tissue and is reported as $E_{dif}$ in the last row of Table 1. Less $E_{dif}$ indicates more uniform tissue differentiation. The BiC fixation resulted in a slightly more uniform differentiation than the MoC fixation for each $X$. For $X = 4$, 6, and 8 pins, $E_{dif}$ was below 0.4 MPa across all tested groups. In contrast, at $X = 2$, $E_{dif}$ exceeded 1 MPa.

Table 1
Difference between the minimum and maximum Young's modulus among the callus elements

| Young's modulus (E) | 2BiC | 2MoC | 4BiC | 4MoC | 6BiC | 6MoC | 8BiC | 8MoC |
|---|---|---|---|---|---|---|---|---|
| $E_{min}$ (MPa) | 3.524 | 3.519 | 4.271 | 4.264 | 4.293 | 4.286 | 4.297 | 4.283 |
| $E_{max}$ (MPa) | 4.527 | 4.53 | 4.669 | 4.663 | 4.667 | 4.661 | 4.666 | 4.657 |
| $E_{dif}$ (MPa) | 1.003 | 1.011 | 0.398 | 0.399 | 0.374 | 0.375 | 0.369 | 0.374 |

# 3. Discussion

Comminuted fractures associated with soft tissue injury and high contamination should be fixed immediately to minimize post-traumatic complications (18). In these cases, external fixators are used as temporary or definitive treatment (19, 20). The goal of this numerical study was to assess the biomechanical and mechano-biological distinction between the bi-cortical and mono-cortical groups of varying pin configurations to treat diaphyseal tibial fractures using unilateral-uniplanar external fixators.

This study shows that the BiC fixations are conducive to higher axial stiffnesses compared with the MoC designs (Fig. 1). It stands to reason the pins in BiC fixation are anchored at two cortices, and bone fragments are displaced less than the MoC group under the applied load. The finding for the relation between the anchored length of the pin and the construct stiffness is consistent with the current literature. Varady et al. (8) performed a clinical test on the porcine tibia fixed by an external fixator and came to the same conclusion. Ochman et al. (21) used locking and non-locking plates to treat metacarpal fractures in domestic pigs and showed that the axial stiffness provided by mono-cortical screws is lower than bi-cortical types. As well, the results observed by Bonner et al. (22) in treating the distal tibial extra-articular fracture were similar to those found here. Of note, the axial stiffness obtained for the MoC system was slightly smaller than the BiC, but both are in the same range (Fig. 1). This result correlates well with that seen in the in-vitro experiment by Mladenovic et al. (4), who found that external fixators mounted by uni-cortical and Schanz pins almost exhibit the same stability in the latero-lateral direction. Even though adding pins makes the construct stiffer, more than four pins did not substantially ameliorate the stiffness. Even though there is always a tendency to employ more pins to create a more stable construct, it should be kept in mind that increasing the number of pins elevates the risk of infection around the pin insertion area (8).

Figure 2 indicates that the mean Young's modulus of the tissue obtained throughout the callus increases by adding pins and enhancing the stiffness of the construct. This effect is rooted in the coherence between the construct stiffness and the pathway of bone healing applied by the mechano-regulation theory of this study (23). Meanwhile, since the difference between the axial stiffness of MoC and BiC groups emerged as negligible (Fig. 1), it was also expected that there would be a slight difference between the mean of Young's modulus within their differentiated tissues. The most noticeable difference was found between the fixators with 2 and 4 pins, which can be explained by the axial stiffness reported for these two models (see Fig. 1).

Fibrous tissue produced at the fracture gap in all models indicated that granulation tissue elements experienced high magnitudes of mechanical stimuli at the initial stage of healing (Fig. 3). This result agrees with the findings of other studies, which showed that mechanical stimulus is higher at the central callus, and fibrocartilage tissue is expected to emerge (23–25). In addition, Fig. 3 shows that for a similar number of pins, the distribution of Young's modulus throughout the callus tissue is accordant in both MoC and BiC cases, given the identical mechanical stiffness provided by both fixation systems.

Although the entire configuration is under an axial vertical load, stiffness mismatch between implant and bone induced bending moment in the fracture zone, while a neutral axis is located outside the bone, closer to a component with higher stiffness, i.e., external fixator. Because of this factor, far cortex callus elements at the far distance from the neutral axis are bent more and tended to be displaced higher than near cortex elements close to the neutral axis (Fig. 4). Based on the mechano-regulation algorithm of bone healing employed in this study, the difference in axial displacements leads to regions with higher and lower Young's modulus at near and far cortices, respectively (Fig. 3). The findings from this study correspond to those of Bottlang *et al.* (26), who conducted a histological evaluation of fracture healing with various locking plate constructs in a sheep tibia. They found that minimal gap motion at the near cortex suppresses fibro-cartilage callus formation.

According to a comparative evaluation of uniformity in different pin configurations illustrated in Table 1, at least four pins are required to achieve a uniform differentiation and even distribution of tissue phenotypes across the callus. Besides, it can be observed that changing the MoC to BiC fixation did not substantially improve the uniformity.

The present computational research incorporated some assumptions and limitations that should be kept in mind when interpreting the results. The models did not realize the threads of pins but instead assumed smooth surfaces tied to the bone tissue at pin-bone interfaces. Considering the fair corroboration that the FE model showed with the in-vitro experiment, this simplifying assumption was inappreciable. Therefore, it cannot be regarded as a significant source of error in this mechano-biological study. However, determining the local effects of pin threads on the stress distribution across the bone cortices awaits further studies. In addition, this study did not investigate pin loosening, one of the challenging problems that depend on the quality of pin-bone interaction. It is worth mentioning that the FE bone model was generated based on the CT images of a healthy adult tibia, which did not suffer from osteoporosis and bone disorders, thus exhibited a dense cortical thickness. Conversely, in patients with skeletal disorders, the risk of cortical bone thinning is escalated (27). Therefore, comparing the BiC and MoC fixations in the occurrence of pin loosening needs a deep consideration of the bone quality. Another parameter that can influence the analyses of this study was the simple transverse fracture geometry with perfectly flat surfaces and a gap size of 3 mm. A broader study that considers the fracture severity and complexity, e.g., oblique, butterfly, and comminuted fractures with irregular shapes and larger gap sizes, could increase the robustness of the FE models and the accuracy of the predicted healing. Moreover, simulations were just limited to the immediate phase of healing, in which the granulation tissue only presents at the fracture gap. Referring to the numerical study by Nourisa and Rouhi (28), we concluded that this limitation does not invalidate the overall reliability of the current results. They showed that the predicted tissue phenotype in the early bone healing stage correlates with the ultimate healing outcome. Nevertheless, it seems that extending the investigations to the entire healing process that could imply periosteal callus formation may likely yield a more rigorous comparison between BiC and MoC fixations.

# 4. Conclusion

The biomechanical and mechano-biological results of this study indicated that MoC fixation is almost equivalent to BiC fixation in treating transverse tibial diaphyseal fractures using the unilateral-uniplanar external fixator. Indeed, since the early fracture reduction resulting from two fixation systems were similar, it appears to be a promising alternative to shift toward using MoC pins in the external fixators; hence, the drawbacks (deep infection, damage to surrounding tissues, and high amount of heat by passing through the bone cortices) of BiC fixations could be discarded.

# 5. Materials And Methods

Two groups of FE models were generated to compare healing outcomes at the early post-operative phase: mono-cortical and bi-cortical. Each group comprised four models fixed by 2, 4, 6, and 8 pins (Fig. 5). Throughout this paper, two terms, *X*MoC and *X*BiC, were defined for brevity, where *X* represents the number of pins, MoC stands for mono-cortical, and BiC means bi-cortical. The different number of pins was intentionally examined in this study to consider its effect on the stiffness and the healing responses of MoC/BiC groups.

# 5.1. Finite element model

A series of 681 computed tomography (CT) images of a 27-year-old healthy woman's left tibia was procured, processed, and converted into point cloud (txt file format) using Mimics Innovation Suite software (V21, Materialise, Belgium). The point cloud file was transferred into the computer-aided design software of Catia (V5.R21, Dassault Systèmes, France) to build a three-dimensional solid model of the intact tibia. Subsequently, a simple transverse fracture with a gap size of 3 mm was embedded in the mid-diaphyseal region of the tibia model according to AO/OTA classification (42-A3). The geometric model of the external fixator was established using specifications given in the implant manufacturer catalog (DePuy Synthes Co., Ltd, New Brunswick, CA, USA). Accordingly, pins with 5 mm diameter and 100 mm length and rod with 8 mm diameter and 350 mm length were designed, assembled, and virtually installed to the anteromedial side of the tibia model. The screw threads were neglected for simplification, but their mechanical and biomechanical effects were considered in the boundary constraints (29). Pins in the MoC group penetrated just into the first bone cortex near the rod, while in the BiC group, they inserted up to the second cortex, far from the rod. The transverse distance of 50 mm was set between the tibial anatomical axis and the longitudinal axis of the rod. The distance between the first pin and the fracture site and between two consecutive pins was 25 mm and 30 mm, respectively. Furthermore, the number of pins was kept identical for proximal and distal fragments of the broken bone.

Since the external periosteal callus does not form at the early stage of healing, only the central callus composed of endosteal and intracortical regions was simulated (30). The geometric models were then imported into Abaqus (V6.14-5, Dassault Systèmes, France) to generate the volumetric mesh. The mesh verification test was carried out using the stiffness criterion, and the optimum mesh size for callus was 1mm, and all other components of the FE model were converged at 2 mm. Table 2 summarizes mesh characteristics for each part in the FE model.

Table 2
Mesh characteristics and material properties used in the FE model (31, 32).

| Part | Young's modulus (MPa) | Poisson's ratio | Element type |
|---|---|---|---|
| Cortical bone | 17000 | 0.3 | C3D10 |
| Cancellous bone | 700 | 0.2 | C3D10 |
| Rod | 200000 | 0.3 | C3D4 |
| Pin | 200000 | 0.3 | C3D8 |
| Callus | 1 (Ref to Table 3) | 0.167 (Ref to Table 3) | C3D10 |

After that, the volumetric mesh was imported into Mimics again to assign the material properties to each bone element. A Hounsfield Unit of 700 was employed to segment contours of cortical and cancellous bone tissues in CT images (15). Pin and rod were considered to be made of stainless steel. All materials were defined as homogeneous, isotropic with linear and elastic mechanical behavior (33, 34). Material properties of the bone and implant components are shown in Table 2.

The remaining FE analysis pre-processing phases were carried out in Abaqus. The fully bonding tie constraints were implemented for describing the interactions between all surfaces in contact, i.e., pin-rod, pin-bone, and callus-bone interfaces (35). Applying the tie constraint is an adequate analytical alternative to compensate for neglected threads and clamps' mechanical and biomechanical effects. According to the AO guideline, a vertical downward load case that equals 20% of body weight for a 75 kg patient was applied as a uniform pressure on the proximal end of the tibia to simulate partial weight-bearing during early post-surgery rehabilitation practice (36). Other loading scenarios were not considered in this study since these forces are not dominant and do not significantly affect the treatment outcome (37). All degrees of freedom were constrained at the distal tibial surface nodes to prevent rigid body motion.

# 5.2. Mechano-regulation algorithm of bone healing

Initially, the entire fracture gap was filled with granulation tissue. A mechano-regulation algorithm (Eq. 1) that has been suggested and validated as an accurate predictive model for the course of bone healing (38) was used to monitor the early differentiation of granulation tissue (14). Accordingly, the deviatoric strain $(\varepsilon_d)$ acts as the mechanical stimulus inside the callus and characterizes the new tissue phenotype (Table 3) (14).

$$\varepsilon_d = \frac{2}{3}\sqrt{(\varepsilon_1-\varepsilon_2)^2+(\varepsilon_1-\varepsilon_3)^2+(\varepsilon_2-\varepsilon_3)^2} \quad (1)$$

where $\varepsilon_1, \varepsilon_2, \text{and } \varepsilon_3$indicate the three principal strains at each callus element. The calculation of the element-wise deviatoric strain and subsequently attributing a new tissue type to each callus element was undertaken by developing a custom Python script.

Table 3
Properties and tissue phenotypes of callus elements classified according to the deviatoric strain theory (14)

| Deviatoric strain () | Tissue type | Young's modulus (MPa) | Poisson's ratio |
|---|---|---|---|
| $\varepsilon_d = 1$ | Granulation tissue | 1 | 0.167 |
| $0.05 \leq \varepsilon_d < 1$ | Fibrous | 1–5 | 0.167 |
| $0.025 \leq \varepsilon_d < 0.05$ | Cartilage | 5-500 | 0.167 |
| $0.0005 \leq \varepsilon_d < 0.025$ | Immature bone | 500–1000 | 0.325 |
| $0.00041 \leq \varepsilon_d < 0.0005$ | Intermediate bone | 1000–2000 | 0.325 |
| $0.00005 \leq \varepsilon_d < 0.00041$ | Mature bone | 2000–6000 | 0.325 |
| $\varepsilon_d < 0.00005$ | Resorption | ---- | ---- |

# 5.3. Validation

The procedure to develop the FE model of fractured tibia-external fixator was indirectly validated against an in-vitro biomechanical study reported in the literature (9). Validation was based on comparing the axial stiffness of the FE construct with the tested model. Axial stiffness was calculated by dividing the applied axial force by the mean axial displacement at the fracture site. In the FE model, all boundary conditions were considered similar to experimental work. The synthetic composite bone tested in that experiment was the fourth-generation, large-sized left tibia, model #3402 (Sawbones; Pacific Research Laboratories Inc., Washington), which had 28 mm width at the mid-shaft and 10 mm diameter at the medullary canal. The corresponding dimensions measured on CT images of the tibia in our study were 29 mm and 11 mm, respectively, which were almost similar to the experimental model.

# Declarations

- **Ethics approval and consent to participate**

Not applicable

- **Consent for publication**

Not applicable

- **Availability of data and materials**

Not applicable

- **Competing interests**

Not applicable

- **Funding**

Not applicable

- **Authors' contributions**

Not applicable

- **Acknowledgements**

We wish to show our gratitude to Dr. Alireza Shakibafard, TABA Medical diagnostic imaging center, for sharing bone CT images with us.

# References

1. Elniel AR, Giannoudis PV. Open fractures of the lower extremity: Current Management and Clinical Outcomes. EFORT open reviews.2018,p.316 – 25, doi: 10.1302/2058-5241.3.170072
2. Hadeed A, Werntz RL, Varacallo M. External fixation principles and overview.2019,p., doi:
3. Meleppuram JJ, Ibrahim S. Experience in fixation of infected non-union tibia by Ilizarov technique–a retrospective study of 42 cases. Revista Brasileira de Ortopedia (English Edition).2017,p.670-5, doi: 10.1016/j.rboe.2016.11.008
4. Mladenovic D, Mitkovic M, Micic I, Karalejic S. Biomechanical Tests and Clinical Application of Unicortical Pin by the External Fixator System. Biotechnology & Biotechnological Equipment.2003,p.136 – 42, doi: 10.1080/13102818.2003.10819209
5. Zhou Y, Wang Y, Liu L, Zhou Z, Cao X. Locking compression plate as an external fixator in the treatment of closed distal tibial fractures. Int Orthop.2015,p.2227–37, doi: 10.1007/s00264-015-2903-7
6. Koettstorfer J, Hofbauer M, Wozasek G. Successful limb salvage using the two-staged technique with internal fixation after osteodistraction in an effort to treat large segmental bone defects in the lower extremity. Arch Orthop Trauma Surg.2012,p.1399 – 405, doi: 10.1007/s00402-012-1564-x
7. Goh J, Thambyah A, Ghani AN, Bose K. Evaluation of a simple and low-cost external fixator. Injury.1997,p.29–34, doi: 10.1016/S0020-1383(96)00149-0
8. Varady PA, Greinwald M, Augat P. Biomechanical comparison of a novel monocortical and two common bicortical external fixation systems regarding rigidity and dynamic stability. Biomedical Engineering/Biomedizinische Technik.2018,p.665 – 72, doi: 10.1515/bmt-2017-0051
9. Ang B, Chen J, Yew A, Chua S, Chou SM, Chia S, et al. Externalised locking compression plate as an alternative to the unilateral external fixator: a biomechanical comparative study of axial and

torsional stiffness. Bone & Joint Research.2017,p.216 – 23, doi: 10.1302/2046-3758.64.2000470

10. Elmedin M, Vahid A, Nedim P, Nedžad R. Finite element analysis and experimental testing of stiffness of the Sarafix external fixator. Procedia Engineering.2015,p.1598 – 607, doi: 10.1016/j.proeng.2015.01.533
11. Krischak GD, Janousek A, Wolf S, Augat P, Kinzl L, Claes LE. Effects of one-plane and two-plane external fixation on sheep osteotomy healing and complications. Clinical Biomechanics.2002,p.470-6, doi: 10.1016/S0268-0033(02)00039-6
12. Roseiro LM, Neto MA, Amaro A, Leal RP, Samarra MC. External fixator configurations in tibia fractures: 1D optimization and 3D analysis comparison. Comput Methods Programs Biomed.2014,p.360 – 70, doi: 10.1016/j.cmpb.2013.09.018
13. Arango D, Tiedeken N, Clippinger B, Samuel SP, Saldanha V, Shaffer G. Biomechanical analysis of four external fixation pin insertion techniques. Orthop Rev (Pavia).2017,p., doi: 10.4081/or.2017.7067
14. Isaksson H, Wilson W, van Donkelaar CC, Huiskes R, Ito K. Comparison of biophysical stimuli for mechano-regulation of tissue differentiation during fracture healing. J Biomech.2006,p.1507–16, doi: 10.1016/j.jbiomech.2005.01.037
15. Zainudin NA, Ramlee MH, Latip HFM, Azaman A, Seng GH, Garcia-Nieto E, et al. Biomechanical evaluation of pin placement of external fixator in treating tranverse tibia fracture: Analysis on first and second cortex of cortical bone. Malaysian Journal of Fundamental and Applied Sciences.2019,p.75 – 9, doi: 10.11113/mjfas.v15n2019.1263
16. Park K-H, Park H-W, Oh C-W, Lee J-H, Kim J-W, Oh J-K, et al. Conventional bicortical pin substitution with a novel unicortical pin in external fixation: A biomechanical study. Injury.2021,p., doi: 10.1016/j.injury.2021.04.036
17. Greinwald M, Varady PA, Augat P. Unicortical self-drilling external fixator pins reduce thermal effects during pin insertion. Eur J Trauma Emerg Surg.2018,p.939 – 46, doi: 10.1007/s00068-017-0887-2
18. Kumar R, Sujai S, Chethan NH, Swamy S. Results of open fractures of tibia treated by external fixator as primary and definitive procedure. Int J Orthop Sci.2017,p.179 – 81, doi: 10.22271/ortho.2017.v3.i1c.30
19. Giannoudis P, Papakostidis C, Roberts C. A review of the management of open fractures of the tibia and femur. The Journal of bone and joint surgery British volume.2006,p.281-9, doi: 10.1302/0301-620X.88B3.16465
20. Garg P, Sodha R, Hamid FB, Somashekarappa T. Clinical Study of Functional Outcome of External Fixator Device as a Primary Definitve Treatment of Open Tibia Fracture. Medico Legal Update.2021,p.768 – 71, doi: 10.37506/mlu.v21i1.2408
21. Ochman S, Doht S, Paletta J, Langer M, Raschke MJ, Meffert RH. Comparison between locking and non-locking plates for fixation of metacarpal fractures in an animal model. The Journal of hand surgery.2010,p.597–603, doi: 10.1016/j.jhsa.2010.01.002
22. Bonner T, Green S, McMurty I, editors. A BIOMECHANICAL COMPARISON OF DIFFERENT SCREW CONFIGURATIONS IN DISTAL TIBIAL LOCKING PLATES. Orthopaedic Proceedings; 2012: The British

Editorial Society of Bone & Joint Surgery.

23. Mohandes Y, Tahani M, Rouhi G, Tahami M. A mechanobiological approach to find the optimal thickness for the locking compression plate: Finite element investigations. Proceedings of the Institution of Mechanical Engineers, Part H: Journal of Engineering in Medicine.2021,p.408 – 18, doi: 10.1177/0954411920985757
24. Ghimire S, Miramini S, Richardson M, Mendis P, Zhang L. Role of dynamic loading on early stage of bone fracture healing. Ann Biomed Eng.2018,p.1768–84, doi: 10.1007/s10439-018-2083-x
25. Carter DR, Beaupré GS, Giori NJ, Helms JA. Mechanobiology of skeletal regeneration. Clinical Orthopaedics and Related Research (1976–2007).1998,p.S41-S55, doi:
26. Bottlang M, Lesser M, Koerber J, Doornink J, von Rechenberg B, Augat P, et al. Far cortical locking can improve healing of fractures stabilized with locking plates. The Journal of Bone and Joint Surgery American volume.2010,p.1652, doi: 10.2106/JBJS.I.01111
27. Rüegsegger P, Durand E, Dambacher M. Localization of regional forearm bone loss from high resolution computed tomographic images. Osteoporos Int.1991,p.76–80, doi: 10.1007/BF01880447
28. Nourisa J, Rouhi G. PREDICTION OF THE TREND OF BONE FRACTURE HEALING BASED ON THE RESULTS OF THE EARLY STAGES SIMULATIONS: A FINITE ELEMENT STUDY. J Mech Med Biol.2019,p.1950021, doi: 10.1142/S0219519419500210
29. Nourisa J, Rouhi G. Biomechanical evaluation of intramedullary nail and bone plate for the fixation of distal metaphyseal fractures. J Mech Behav Biomed Mater.2016,p.34–44, doi: 10.1016/j.jmbbm.2015.10.029
30. Eastaugh-Waring S, Joslin C, Hardy J, Cunningham J. Quantification of fracture healing from radiographs using the maximum callus index. Clinical Orthopaedics and Related Research®.2009,p.1986-91, doi: 10.1007/s11999-009-0775-0
31. Duda GN, Mandruzzato F, Heller M, Goldhahn J, Moser R, Hehli M, et al. Mechanical boundary conditions of fracture healing: borderline indications in the treatment of unreamed tibial nailing. J Biomech.2001,p.639 – 50, doi: 10.1016/S0021-9290(00)00237-2
32. Isaksson H, Van Donkelaar CC, Ito K. Sensitivity of tissue differentiation and bone healing predictions to tissue properties. J Biomech.2009,p.555 – 64, doi: 10.1016/j.jbiomech.2009.01.001
33. Qiu T-X, Teo E-C, Yan Y-B, Lei W. Finite element modeling of a 3D coupled foot–boot model. Med Eng Phys.2011,p.1228–33, doi: 10.1016/j.medengphy.2011.05.012
34. Jafari B, Ashjaee N, Katoozian H, Tahani M. A comparative study of bone remodeling around hydroxyapatite-coated and novel radial functionally graded dental implants using finite element simulation. Med Eng Phys.2022,p.103775, doi:
35. Nourisa J, Baseri A, Sudak L, Rouhi G. The effects of bone screw configurations on the interfragmentary movement in a long bone fixed by a limited contact locking compression plate. J Biomed Sci Eng.2015,p.590, doi:
36. Ruedi TP. AO principles of fracture management2000.

37. Taylor M, Tanner K, Freeman M, Yettram A. Stress and strain distribution within the intact femur: compression or bending? Med Eng Phys.1996,p.122 – 31, doi:
38. Isaksson H, Van Donkelaar CC, Huiskes R, Ito K. Corroboration of mechanoregulatory algorithms for tissue differentiation during fracture healing: comparison with in vivo results. J Orthop Res.2006,p.898–907, doi:

# Figures

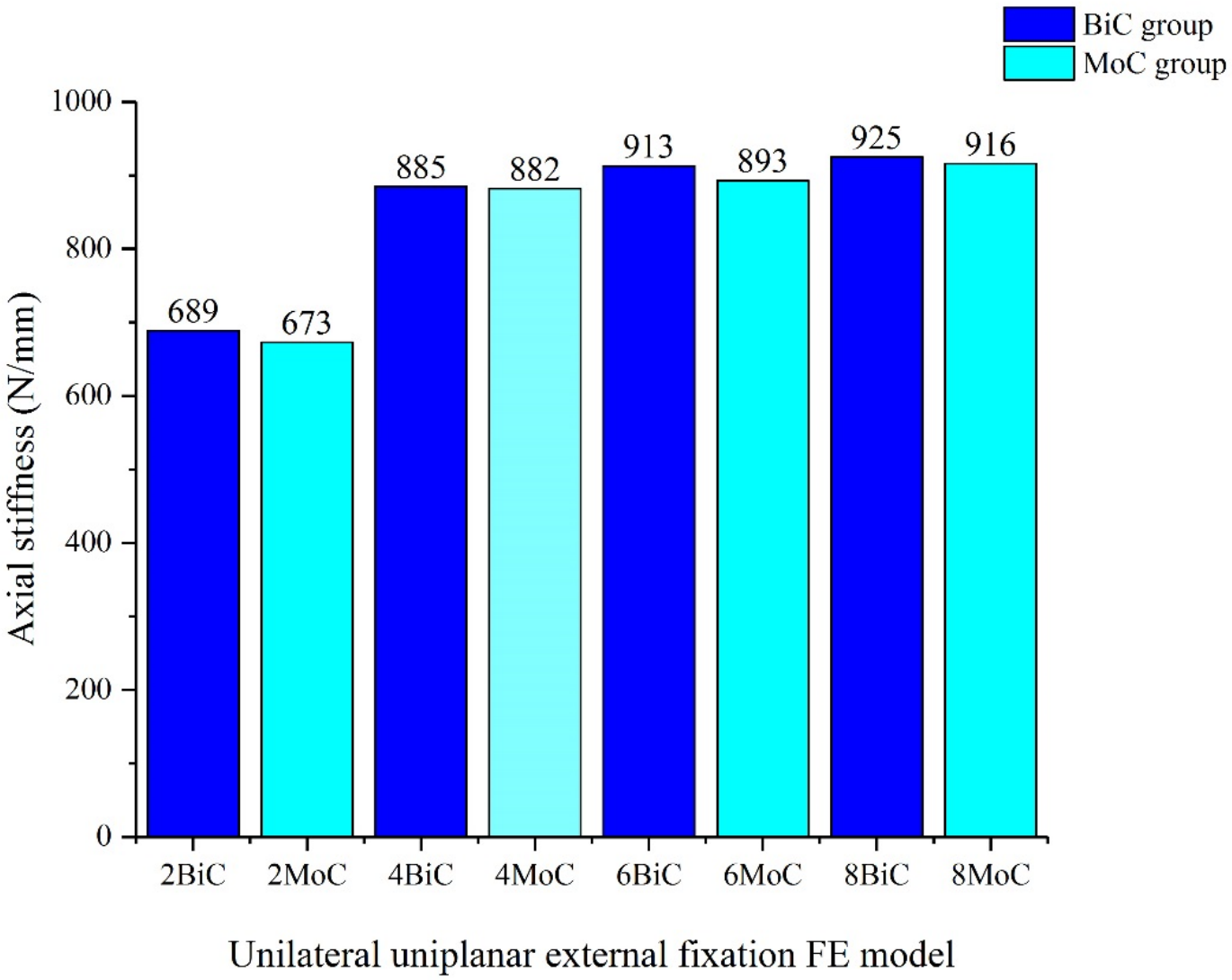


**Figure 1**

The overall axial stiffness for eight FE models in BiC and MoC groups

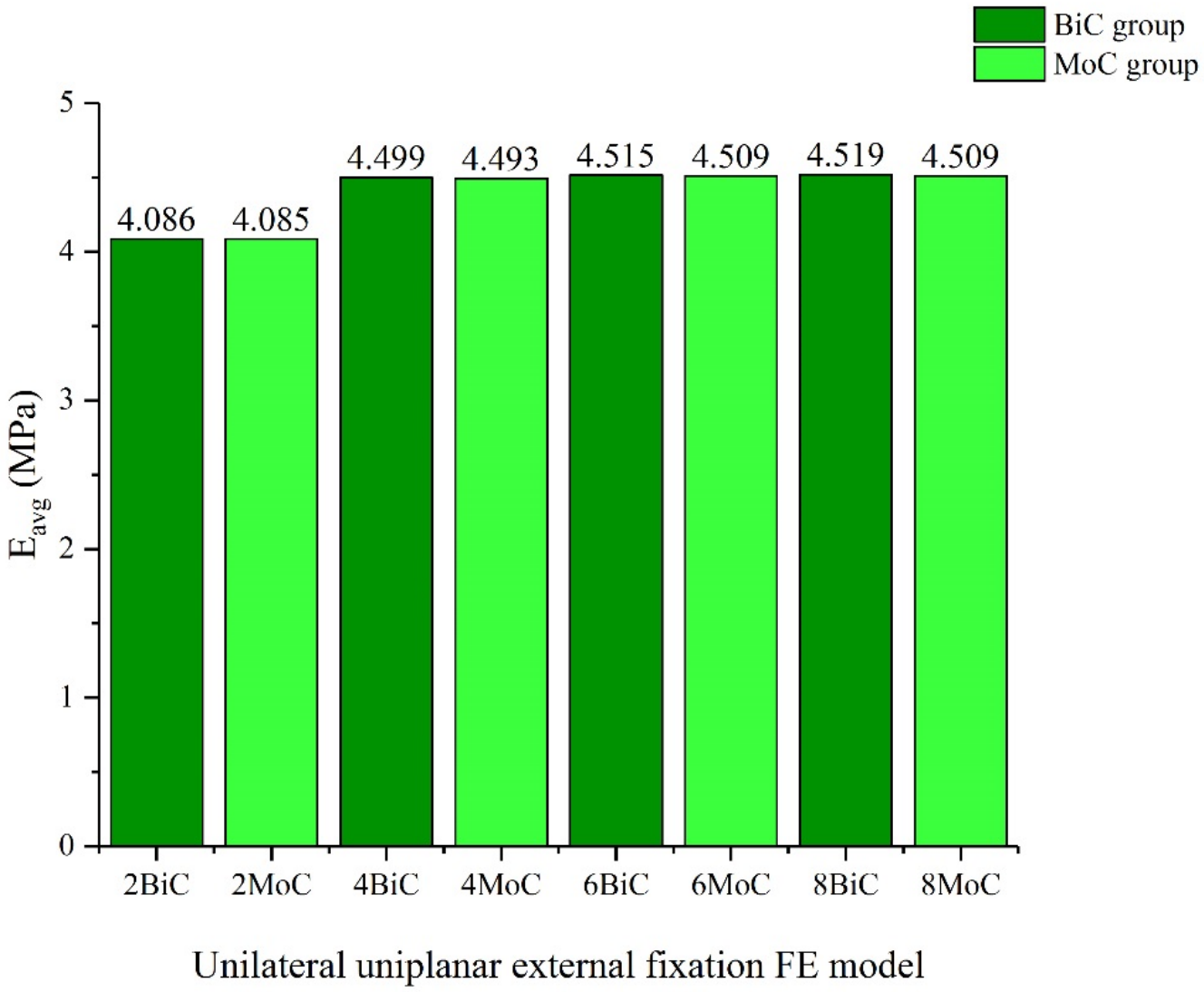


**Figure 2**

The average Young's modulus of callus elements in eight FE models in BiC and MoC groups

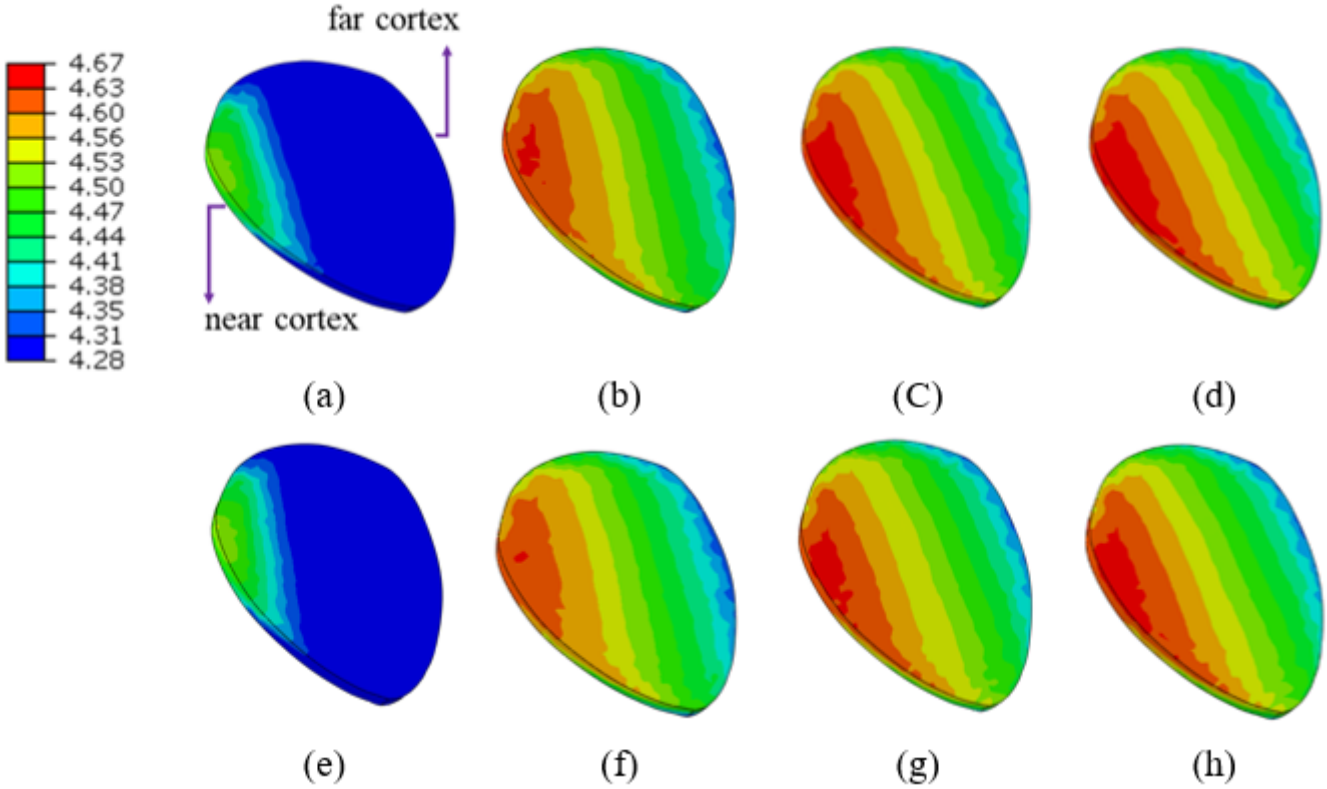


## Figure 3

Young's modulus (MPa) contour plot in callus for fixation models: (a) 2BiC; (b) 4BiC; (c) 6BiC; (d) 8BiC; (e) 2MoC; (f) 4MoC; (g) 6MoC; (h) 8MoC.

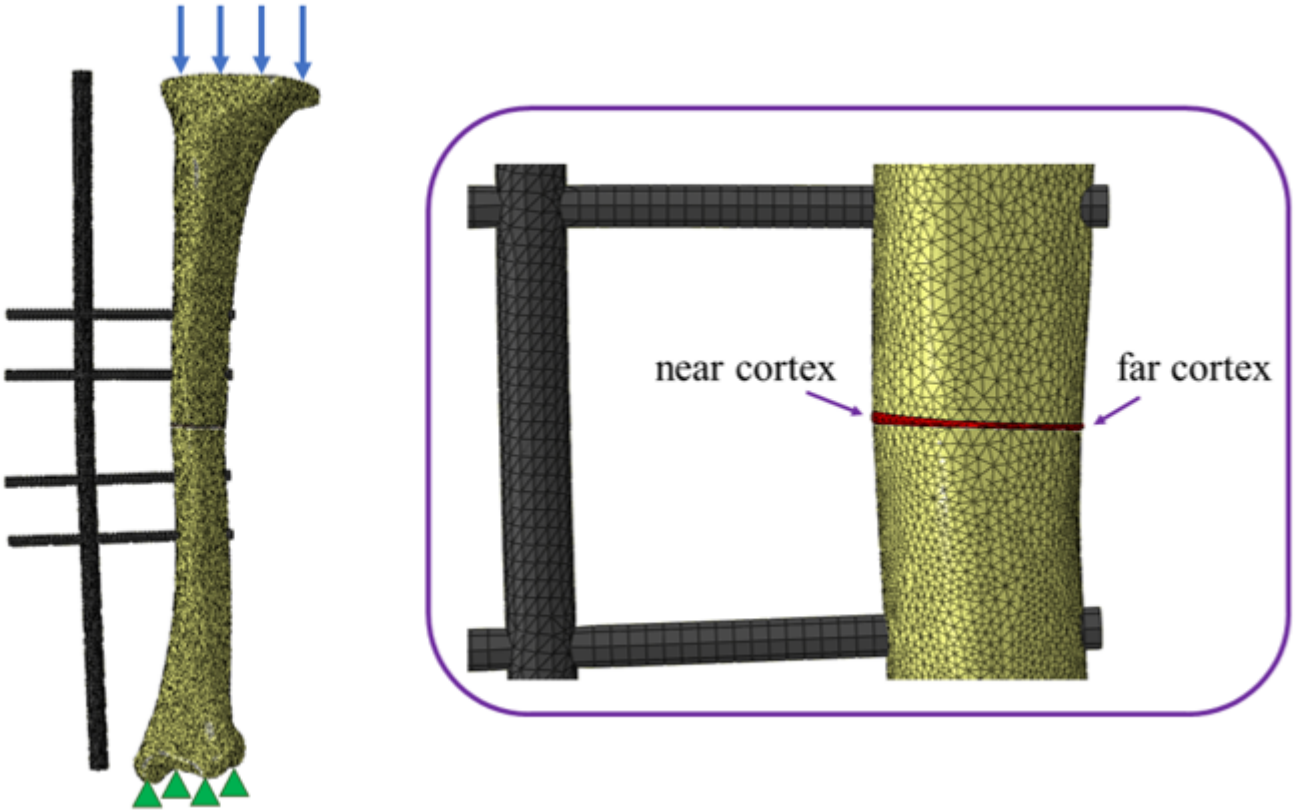


**Figure 4**

Near and far cortex callus elements realize different displacements due to the bending induced at the fracture site.

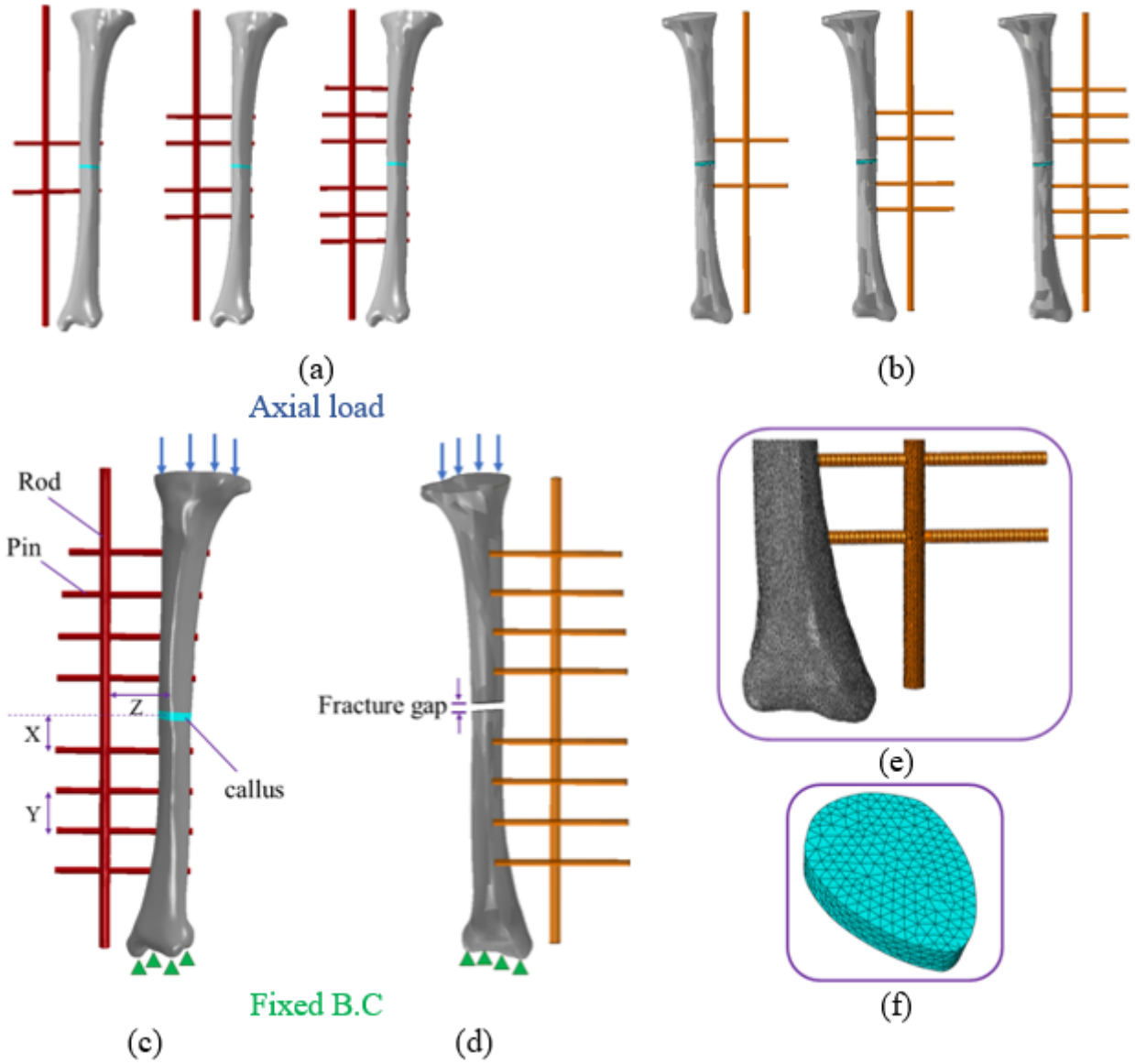


## Figure 5

**(a)** The bi-cortical group including 2BiC, 4BiC, 6BiC; **(b)** the mono-cortical group including 2MoC, 4MoC, 6MoC; **(c), (d)** illustration of vertical downward load acted on the proximal end, and restrained boundary condition at the distal end of a sample construct with eight pins: 8BiC and 8MoC. Distance of the nearest pin to fracture site, the distance between consecutive pins, and rod elevation were labeled as X, Y, and Z respectively; **(e)** a close-up view of finite element mesh generated on the tibia, rod, and pin.; **(f)** discretized model of central callus composed of endosteal and intercortical regions, generated on the tibia, rod, and pin.